# Pre-tightening Force Analysis of a Pre-stressed Six-axis Force Sensor

Zhijun Wang[1, 2]
1. College of Mechanical Engineering Hebei United University, Tangshan, China
2. Hebei Provincial Key Laboratory of Parallel Robot and Mechatronic System, Yanshan University
Qinhuangdao, China
e-mail: zjwang@heuu.edu.cn

Jing He
Tangshan Industrial Vocational Technical College
Tangshan, China
e-mail: hejing409@126.com

Wanyu Liu
College of Mechanical Engineering
Hebei United University,
Tangshan, China
e-mail: 454283817@qq.com

Yongsheng Zhao
Hebei Provincial Key Laboratory of Parallel Robot and Mechatronic System, Yanshan University
Qinhuangdao, China
e-mail: yszhao@ysu.edu.cn

**Abstract—By using sphere pair with unilateral constraint, the limbs of the proposed pre-stressed six-axis sensor must be under pressure in the measurement process, so prior to measurement, a certain preload must be applied to the sensor. The viable limbs' number of the pre-stressed six-axis force senor is determined by using convex theorem. By solving the static equilibrium equation of sensor, the reacting forces on limbs are divided into two parts: the particular solution is generated by the external force, while the homogeneous solution is only concerned with the pre-tightening force. The number of parameters to be determined in homogeneous solution is decreased by linear transform, and the method for determining the pre-tightening force is derived to make all the limbs compressed when it is subjected to the expected range of external force. A numerical example to determine the pre-tightening force of the force sensor is performed. The numerical example results show that the force on limbs can always maintain positive value with the appropriate pre-tightening force, which proves the correctness of the theoretical analysis and the validity of the sensor structure.**

***Keywords-component; Force sensor; Six-axis; Pre-stressed; Pre-tightening force; Reacting force***

## I. INTRODUCTION

With the ability of measuring three force components and three torque components applied to the end-effector, the six-axis force/torque sensor is one kind of the most important and challenging sensors, which is widely used in both industries and research as well, and real-time measurement of six-axis force/torque is a foundation to realize force compliance control and multi-degree-freedom- coordinated control on industrial robots. The trend of industrial automation increasingly requires the use of robotic manipulators with force/torque sensor to serve works such as rehabilitation, welding, grinding, deburring, object gripping and moving, etc.

Parallel mechanisms possess the distinguishing advantages of high rigidity, symmetry and stress decoupling that make them particularly suitable for certain applications in multi-axis force/torque sensors. A lot of literatures on the design, analysis, and optimization of the parallel six-axis force/torque sensor with static or hyperstatic structure are available in recent years. Gaillet and Reboulet [1] proposed an isostatic six-axis force/torque sensor based on the octahedral structure of the Stewart platform. Kerr [2] suggested that the Stewart platform with instrumented elastic legs be used as a six-axis force/torque sensor and enumerated a few design criteria for the sensor structure. Dasgupta et al. [3] presented a design methodology for the Stewart platform sensor structure based on the optimal conditioning of the force transformation matrix. Jin et al. [4] proposed a unique design of a six-component force/torque sensor and analyzed the translational stiffness and the torsional stiffness. Dwarakanath et al. [5, 6] presented a simply supported, „joint less" six-component parallel mechanism-based force/torque sensor. Hou et al. [7] proposed a hyperstatic six-axis force/torque sensor based on Stewart platform, and discussed the performance analysis and comprehensive index optimization of the six-axis force sensor. Another kind of six-axis force/torque sensor is unitary structure based on strain gauge bridge, which has the advantages of high rigidity, miniaturization, compact structure, etc. Huang et al. [8] performed the mechanical analysis of a novel six-degree-of-freedom wrist force/torque sensor with a simple structure and small cross-sensitivity. Liu et al. [9] presented a six-axis parallel force sensor for human dynamics analysis and adopted finite element method to optimize mechanism dimension of the force sensor. Kim et al. [10, 11] developed a six-axis force/torque sensor to use as an intelligent robot"s gripper for safely grasping an unknown object and accurately perceiving the position of the object in the grippers.

For the pre-stressed force/torque sensor with a certain pre-tightening force, the measurement range is the limit force/ torque that can be applied on the measuring platform while all the limbs are in the state of compressed. So when the measurement range is known, determination of the pre-tightening force is the key in establishing a design procedure. Having external force calculated as a function of the axial force on limbs, the problem is reduced to adjusting initial condition by selecting a proper pre-tightening force so that all the axial forces of the limbs are always **c**ompressed.

## II. Determination of the Measuring Limbs" Number

To improve the traditional Stewart force sensor, a cone-shaped spherical pairs with unilateral constraint is used to connect the measuring limb and the platforms instead of the traditional sphere pairs. The unilateral constraint of cone-shaped spherical pairs is similar to the frictionless point contact. So if the sensor wants to resist any external force, it must be in the state of force-closure. Moreover, the pattern of force-closure is determined by the number of the sensor"s measuring limbs. For the pre-stressed six-axis force sensor, upper and lower bounds for the number of measuring limbs required for a force-closure constraint can be obtained by using two classical theorems in convex analysis.

**Theorem 1** (Caratheodory). If a set $\boldsymbol{X}=\{v_1,\ v_2,\ ...,\ v_k\}$ positively spans $\boldsymbol{R}^p$, then $k \geq p+1$.

**Theorem 2** (Steinitz). If $\boldsymbol{S} \subset \boldsymbol{R}^p$ and $q \in \operatorname{int}(\operatorname{co}\boldsymbol{S})$, then there exists $\boldsymbol{X}=\{v_1,\ v_2,\ ...,\ v_k\} \subset \boldsymbol{S}$ such that $q \in \operatorname{int}(\operatorname{co}\boldsymbol{X})$ and $k \leq 2p$. Let $\operatorname{co}\boldsymbol{S}$ denote the convex hull of a set $\boldsymbol{S}$, $\operatorname{int}(\operatorname{co}\boldsymbol{S})$ denote the interior of the convex hull.

**Theorem 1** and **Theorem 2** allow us to bound the number of contacts required for a force-closure grasp using frictionless point contacts. Caratheodory"s theorem implies that if a rigid body can be restricted with a force-closure state, then it must have at least $p$+1 unilateral contacts. And Steinitz"s theorem places an upper bound on the minimal number of unilateral contacts which are needed. For a rigid body in three-dimensional space, the applied external force is six-dimensional (three-dimensional force and three-dimensional torque), so at least seven and at most twelve measuring limbs will be available in order to restrict the measuring platform in the state of static balance. Considering that the structure of the sensor may be as simple and Symmetric as possible to reduce the error source, eight measuring limbs are chosen to the design in this paper.

## III. Structure Characteristics of the Pre-Stressed Six-Axis Force Sensor

The pre-stressed six-axis force sensor based on modified Stewart platform with dual layers architecture is shown in Fig .1. It is composed of pre-stressing platform, measuring platform, base platform, pre-stressing bolts and eight measuring limbs. Each measuring limb is a high performance single-axis force transducer to ensure the accuracy of the six-axis force sensor system. The pre-tightening force is applied to the pre-stressing platform and base platform by pre-stressing bolts in order to hold down all the limbs before measuring. The measuring limbs are divided into two layers, four measuring limbs are placed above the measuring platform, and other four limbs are placed below the measuring platform. As the unilateral constraint of cone-shaped spherical pairs, it must insure that all the measuring limbs are always compressed in the measuring process, so a certain pre-tightening force must apply on the measuring limbs.

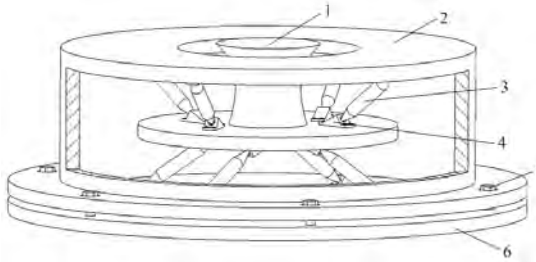


1.measuring platform, 2.pre-stressing platform, 3. measuring limb, 4.ball socket, 5. pre-stressing bolt, 6. base platform

Figure 1. The pre-stressed six-axis force sensor with dual layers

Besides the advantages of lower joint frictional moment, lower nonlinearity and mechanical hysteresis, convenient series products etc, the pre-stressed and dual layers architecture force sensor proposed in this paper has several additional advantages to improve the superiority of pre-stressed parallel structure. The dynamic stiffness of the sensor will be much more improved with the action of the pre-tightening force. It can endure more rotational torque due to the measuring limbs placed at both sides of the measuring platform. The sensor structure is symmetrical. Furthermore, the infliction way of the pre-tightening force can ensure the condition of pre-stressed more safety and stability.

## IV. Pre-Tightening Force Analysis

### A. *Static mathematical model*

As the foundation for hyperstatic analysis, the static mathematical model of the six-axis force/torque sensor should be built firstly. As shown in Fig .2, the Cartesian coordinate system $o$-$xyz$ is set up with its origin coinciding with the underside geometric center of the measuring platform. And the symbols are defined as follows: $\boldsymbol{b}_i$ and $\boldsymbol{B}_i$ ( $i$=1, 2, 3, 4) denote the position vectors of the $i$th spherical joint of the upside of the measuring platform and the pre-stressing platform about the coordinate system, and $\boldsymbol{b}_j$ and $\boldsymbol{B}_j$ ($j$=5,6,7, 8) denote the position vectors of the $j$th spherical joint of the underside of the measuring platform and the base platform. $R$ denotes the radii of the circle, with which the center of spherical joint located on the pre-stressing platform and base platform, $r$ denotes the radii of the circle of the measuring platform, and $l$ denotes the length of the measuring limb. $H$ is the distances between the pre-stressing or base platform and the upside of the measuring platform. $h$ denotes the height from upside to underside of the measuring platform. $\alpha$ , $\beta$ and $\gamma$ denote the central angle of the spherical joint ($b_1$) of the upside of the measuring platform, the spherical joint ($B_5$) of the base platform and the spherical joint ($B_1$) of the pre-stressing platform with respect to $x$-axis of the coordinate system, respectively.

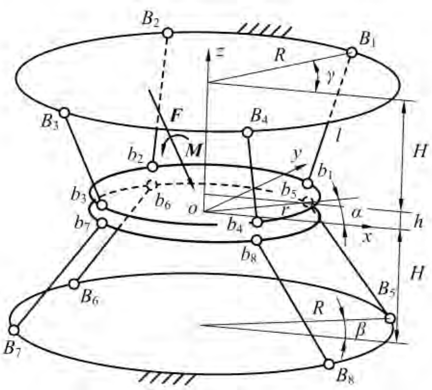


Figure 2. Schematic drawing of the pre-stressed six-axis force/torque sensor.

For the equilibrium of the measuring platform, the following equation can be obtained as

$$\boldsymbol{F} = \boldsymbol{G} \cdot \boldsymbol{f} \tag{1}$$

where $\boldsymbol{F} = [F_x \quad F_y \quad F_z \quad M_x \quad M_y \quad M_z]^{\mathrm{T}}$ is the vector of six-dimension force applied on the center of measuring platform; $\boldsymbol{f} = [f_1 \quad f_2 \quad f_3 \quad f_4 \quad f_5 \quad f_6 \quad f_7 \quad f_8]^{\mathrm{T}}$ is the vector composed of the forces of the eight limbs; $\boldsymbol{G}$ is the force Jacobin matrix.

If the rank of matrix $[\boldsymbol{G}]$ equates to the rank of matrix $[\boldsymbol{G} \quad \boldsymbol{F}]$, the solution to Eq. (1) can be obtained as follows.

$$\boldsymbol{f} = \boldsymbol{G}^{-}\boldsymbol{F} + \left(\boldsymbol{I} - \boldsymbol{G}^{-}\boldsymbol{G}\right)\boldsymbol{y} \tag{2}$$

where $\boldsymbol{G}^{-}$ is the 8×6 generalized inverse matrix for the 6×8 active statics Jacobian matrix, and the matrix of $\boldsymbol{G}^{-}$ is not unique. $\boldsymbol{I}$ is the 8×8 identity matrix. $\boldsymbol{y} = \left[y_1 \quad y_2 \quad \ldots \quad y_8\right]^{\mathrm{T}}$ is a 8-dimensional arbitrary vector.

Eq.(2) is made up of two parts: the particular solution $\boldsymbol{f}_{\mathrm{p}}$ and the homogeneous solution $\boldsymbol{f}_{\mathrm{h}}$

$$\boldsymbol{f}_{\mathrm{p}} = \boldsymbol{G}^{-}\boldsymbol{F} \tag{3}$$

$$\boldsymbol{f}_{\mathrm{h}} = \left(\boldsymbol{I} - \boldsymbol{G}^{-}\boldsymbol{G}\right)\boldsymbol{y} \tag{4}$$

We define that the forces on limbs are positive when the limbs are compressed. So, the value of $\boldsymbol{f}$ in Eq. (1) must be positive when a measured force applied to the sensor. From Eqs. (3) and (4), it can be seen that the forces of the eight limbs are divided into two parts. The particular solution $\boldsymbol{f}_{\mathrm{p}}$ is produced by the external force, while the homogeneous solution $\boldsymbol{f}_{\mathrm{h}}$ is not related to the external force but the pre-tightening force.

In Eq. (2), the particular solution equation $\boldsymbol{f}_{\mathrm{p}}$ is the least-squares solution to achieve the desired wrench, and the homogeneous solution $\boldsymbol{f}_{\mathrm{h}}$ projects $\boldsymbol{y}$ into the null space of $\boldsymbol{G}^{-}$. So in principle the Eq. (4) may be used to increase limb stresses until all measuring limbs are compressed when the sensor is subjected to the expected range of external loads. It can be seen that the forces of pre-tightening are not related to external force, but the internal forces of the hyperstatic structure. So we can define the pre-tightening force as the homogeneous solution $\boldsymbol{f}_{\mathrm{h}}$, which is only related to the vector $\boldsymbol{y}$ in Eq.(4) when the architecture of sensor is determined. Then the problem of determining the pre-tightening force can be formulated as the quantity of the vector $\boldsymbol{y}$.

### *B. Maximum reacting force on limbs*

In order to ensure that all the measuring limbs are always in compression, which limb generated the maximum of reacting force when subjected to the expected range of external loads will be evaluated firstly. Eq. (3) expresses the mathematical relationship between the external force and the reacting force on limbs

$$\boldsymbol{f}_{\mathrm{p}} = \boldsymbol{C}\ \boldsymbol{F} \tag{5}$$

where $\boldsymbol{C} = \boldsymbol{G}^{-}$.

For a general six-axis force/torque sensor, the measuring range can be given as the maximal magnitudes on the six axes $F_{\mathrm{xm}}, F_{\mathrm{ym}}, F_{\mathrm{zm}}$, $M_{\mathrm{xm}}, M_{\mathrm{ym}}, M_{\mathrm{zm}}$. Based on the discussion above, the maximum reacting forces on limbs are deduced in the following analysis by solving inequations.

Separation of reacting force on the *i*-th limb of the sensor, the following result can be produced

$$\begin{aligned} \left|f_{\mathrm{p}i}\right| &= \left|C_{i1}F_{\mathrm{x}} + C_{i2}F_{\mathrm{y}} + C_{i3}F_{\mathrm{z}} + C_{i4}M_{\mathrm{x}} + C_{i5}M_{\mathrm{y}} + C_{i6}M_{\mathrm{z}}\right| \\ &\le \left|C_{i1}F_{\mathrm{x}}\right| + \left|C_{i2}F_{\mathrm{y}}\right| + \left|C_{i3}F_{\mathrm{z}}\right| + \left|C_{i4}M_{\mathrm{x}}\right| + \left|C_{i5}M_{\mathrm{y}}\right| + \left|C_{i6}M_{\mathrm{z}}\right| \\ &\le \left|C_{i1}F_{\mathrm{xm}}\right| + \left|C_{i2}F_{\mathrm{ym}}\right| + \cdots + \left|C_{i6}M_{\mathrm{zm}}\right| = \max\left|f_{\mathrm{p}i}\right| \end{aligned} \tag{6}$$

where $|\cdot|$ represents the absolute value of the corresponding expression, $f_{\mathrm{p}i}$ is the particular solution component of reacting force on the *i*-th limb, $\max\left|f_{\mathrm{p}i}\right|$ denotes the maximum of reacting force on the *i*-th limbs when the permissible force applied on the sensor, and $C_{ij}\left(i = 1,2,...,8, \quad j = 1,2,...,6\right)$ is the element at the *i*-th row and the *j*-th column of matrix $\boldsymbol{C}$.

Obviously, the reacting force on the *i*-th limb gets maximal value both only if the external force gets maximal value, and relates to the positive and negative of the coefficient $C_{ij}$. This is because the space models of the permissible external force are convex.

### *C. Determination of the pre-tightening force* $\boldsymbol{f}_{\mathrm{h}}$

If the space model of the permissible external force is symmetrical about the origin, the reacting force on the *i*th limb $f_{\mathrm{p}i}$ in Eq. (5) can be limited as

$$-\max\left|f_{\mathrm{p}i}\right| \le f_{\mathrm{p}i} \le \max\left|f_{\mathrm{p}i}\right| \tag{7}$$

We will adjust the arbitrary vector $\boldsymbol{y}$ in Eq. (2) to make sure that the forces $\boldsymbol{f}$ are always positive when the external force of measuring range is applied on the sensor. But $\boldsymbol{y}$ is a 8-dimensional vector which contains eight parameters to be determined, the following transformation is introduced to reduce the unknown parameters.

Suppose that $\boldsymbol{u}_1$ and $\boldsymbol{u}_2$ are the independent column vector, and then the column vector in matrix $(\boldsymbol{I}-\boldsymbol{G}^{-}\boldsymbol{G})$ can be expressed as

$$\boldsymbol{\omega}_i = \lambda_{i1}\boldsymbol{u}_1 + \lambda_{i2}\boldsymbol{u}_2 \quad (i = 1, 2, \cdots, 8) \tag{8}$$

where $\boldsymbol{\omega}_i$ is the $i$-th column vector in matrix $(\boldsymbol{I}-\boldsymbol{G}^{-}\boldsymbol{G})$, $\lambda_{i1}, \lambda_{i2}$ is the vector of linear transformation.

Substituting Eq. (8) into Eq. (4), obtains

$$\begin{aligned} \boldsymbol{f}_{\mathrm{h}} &= (\boldsymbol{\omega}_1, \boldsymbol{\omega}_2, \cdots, \boldsymbol{\omega}_8)(y_1 \quad y_2 \quad \cdots \quad y_8)^{\mathrm{T}} \\ &= (\lambda_{11}\boldsymbol{u}_1 + \lambda_{12}\boldsymbol{u}_2, \cdots, \lambda_{81}\boldsymbol{u}_1 + \lambda_{82}\boldsymbol{u}_2)(y_1 \quad \cdots \quad y_8)^{\mathrm{T}} \\ &= y_1(\lambda_{11}\boldsymbol{u}_1 + \lambda_{12}\boldsymbol{u}_2) + \cdots + y_8(\lambda_{81}\boldsymbol{u}_1 + \lambda_{82}\boldsymbol{u}_2) \\ &= \sum_{i=1}^{8} y_i\lambda_{i1}\boldsymbol{u}_1 + \sum_{i=1}^{8} y_i\lambda_{i2}\boldsymbol{u}_2 = k_1\boldsymbol{u}_1 + k_2\boldsymbol{u}_2 \end{aligned} \tag{9}$$

where $k_1, k_2$ are arbitrary numerical value.

Combining Eqs. (2), (5) and (9), we have

$$\boldsymbol{f} = \boldsymbol{G}^{-}\boldsymbol{F} + k_1\boldsymbol{u}_1 + k_2\boldsymbol{u}_2 \tag{10}$$

Make sure that the forces $\boldsymbol{f}$ are always positive, Eq. (10) is always greater than zero vector, then

$$\boldsymbol{G}^{-}\boldsymbol{F} + k_1\boldsymbol{u}_1 + k_2\boldsymbol{u}_2 > \boldsymbol{0} \tag{11}$$

Solving the inequation, the pre-tightening force can be obtained by determination of $k_1, k_2$. It can be concluded that if the pre-tightening force is greater than the critical value of $k_1\boldsymbol{u}_1 + k_2\boldsymbol{u}_2$ in Eq. (9), all the measuring limbs will be compressed when the sensor is subjected to the expected range of external loads.

## V. NUMERICAL EXAMPLE

For the pre-stressed six-axis force/torque sensor, force transmission performance is closely related to the seven structural parameters, which include the radii of the base platform and pre-stressing platform $R$, the radii of the measuring platform $r$, the height $l$, $h$, the directional angles $\alpha$, $\beta$ and $\gamma$. The preliminary values of the structural parameters are given as below:

$r = 25\,\mathrm{mm}$, $R = 40\,\mathrm{mm}$, $h = 9\,\mathrm{mm}$, $l = 31\,\mathrm{mm}$, $\alpha = \pi/4$, $\beta = \pi/6$, $\gamma = \pi/3$.

According to the structural parameters, the corresponding force Jacobin matrix can be calculated as

$$\boldsymbol{G} = \begin{bmatrix} -0.078 & 0.078 & 0.078 & -0.078 & -0.570 & 0.570 & 0.570 & -0.570 \\ -0.570 & -0.570 & 0.570 & 0.570 & -0.078 & -0.078 & 0.078 & 0.078 \\ -0.817 & -0.817 & -0.817 & -0.817 & 0.817 & 0.817 & 0.817 & 0.817 \\ -0.009 & -0.009 & 0.009 & 0.009 & 0.014 & 0.014 & -0.014 & -0.014 \\ 0.013 & -0.013 & -0.013 & 0.013 & -0.014 & 0.014 & 0.014 & -0.014 \\ -0.008 & 0.008 & -0.008 & 0.008 & 0.008 & -0.008 & 0.008 & -0.008 \end{bmatrix} \tag{12}$$

Suppose that the maximal magnitudes of expected external force are given as $F_{\mathrm{xm}} = F_{\mathrm{ym}} = F_{\mathrm{zm}} = 250\mathrm{N}$, $M_{\mathrm{xm}} = M_{\mathrm{ym}} = M_{\mathrm{zm}} = 20\mathrm{Nm}$, then by Eq. (6) the maximum of particular solution component of reacting force is

$$\begin{cases} f_{\mathrm{Rm}i} = 888.13\,\mathrm{N} & (i = 1, 2, 3, 4) \\ f_{\mathrm{Rm}j} = 847.46\,\mathrm{N} & (j = 5, 6, 7, 8) \end{cases} \tag{13}$$

And then solving the inequation of Eq. (11), we obtain

$$k_1 > 888, \quad k_2 > 554 \tag{14}$$

Substituting the critical value of $k_1, k_2$ into Eq. (9), then the pre-tightening force can be expressed as follows

$$\boldsymbol{f}_{\mathrm{h}} > [0.89 \quad 0.55 \quad 0.89 \quad 0.55 \quad 0.89 \quad 0.55 \quad 0.89 \quad 0.55]^{\mathrm{T}}\,\mathrm{N} \tag{15}$$

Fig .3 illustrates the calculation results of how the forces on limbs change their magnitudes with respect to the arbitrary numerical value $k_1, k_2$ Obviously, it can be seen that when $k_1 > 888, k_2 > 554$, all the forces on limbs $f_1$ and $f_8$ are positive and present linear increase with $k_1$ and $k_2$. Further, the Surface in Fig .3 show that in order to make the force on limbs always maintain positive value, the magnitude of $k_1$ must be greater than 888, while $k_2$ greater than 554.

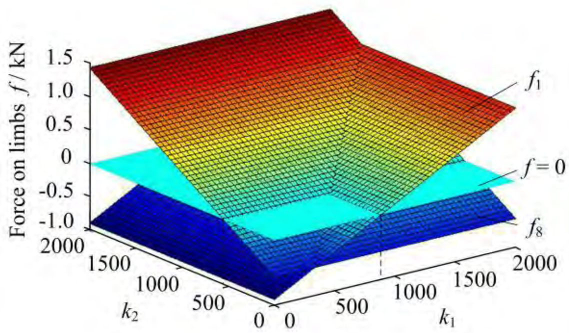


Figure 3. Results of the force on limbs with respect to $k_1$ and $k_2$.

## VI. CONCLUSIONS

In this paper, the pre-tightening force analysis of a pre-stressed six-axis force/torque sensor with double layers have been conducted. In principle, by using the cone-shaped spherical pairs instead of the traditional sphere pairs, the proposed pre-stressed six-axis force/torque sensor has the advantages of high rigidity, low nonlinearity and mechanical hysteresis, safe and steady structure and so on. By using convex theorem, for the force/torque sensor, the applied external force is six-dimensional (three-dimensional force and three-dimensional torque), so at least seven and at most twelve measuring limbs will be available in order to restrict the measuring platform in the state of static balance. With the aim of minimizing the maximum reacting force of measuring limbs when applied a predefined task, a linear transformation method is presented to determine the pre-tightening force. The structural parameters of the sensor are obtained by mapping the relationship between the maximum forces of measuring limbs and the structural parameters. Finally, the numerical example is carried out. It shows that the force on limbs can always maintain positive value with the appropriate pre-tightening force, which proves the correctness of the theoretical analysis and the validity of the sensor structure. The contents of this paper should be useful for the further research of the pre-stressed six-axis force/torque sensor.


## ACKNOWLEDGMENT

This work is supported by the Scientific Research Foundation of Hebei Provincial Education No. QN20131105.


## REFERENCES


[1] A. Gaillet and C. Reboulet, "An isostatic six component force and torque sensor, in: Proceedings of the 13th International Symposium on Industrial," Robotics, 1983, pp. 102-111.

[2] D. R. Kerr, "Analysis, properties and design of a Stewart-platform transducer," ASME, Design Engineering Division, Trends and Developments in Mechanisms, Machines, and Robotics. vol. 15, 1988, pp. 139-145.

[3] B. Dasgupta, S. Reddy and T.S. Mruthyunjaya, "Synthesis of a Force-Torque Sensor Based on the Stewart Platform Mechanism," In: Proceedings of the National Convention of Industrial Problems in Machines and Mechanisms (IPROMM'94), Bangalore, India, 1994, pp. 14−23.

[4] Z. L. Jin, F. Gao and X. H. Zhang, "Design and analysis of a novel isotropic six-component force/torque sensor," Sensors and Actuators A, vol. 109, 2003, pp. 17-20.

[5] T. A. Dwarakanath, B. Dasgupta and T. S. Mruthyunjaya, "Design and development of a Stewart platform based force-torque sensor," Mechatronics, vol. 11, 2001, pp. 793-809.

[6] T. A. Dwarakanath and D. Venkatesh, "Simply supported, „Joint less" parallel mechanism based force-torques sensor," Mechatronics, vol. 16, 2006, pp. 565-575.

[7] Y. L. Hou, J. T. Yao, L. Lu and Y .S. Zhao, "Performance analysis and comprehensive index optimization of a new configuration of Stewart six-component force sensor," Mechanism and Machine Theory, vol. 44, 2009, pp. 359-368.

[8] W. Y. Huang, H. M. Jiang and H. Q. Zhou, "Mechanical analysis of a novel six-degree-of-freedom wrist force sensor," Sensors and Actuators A, vol. 35, 1993, pp. 203-208.

[9] T. Liu, Y. Inoue, K. Shibata, Y. Yamasaki and M. Nakahama, "A six-dimension parallel force sensor for human dynamics analysis," In: 2004 IEEE Conference on Robotics, Automation and Mechatronics, Singapore, December 2004, pp. 208-212.

[10] G. S. Kim, "Design of a six-axis wrist force/moment sensor using FEM and its fabrication for an intelligent robot," Sensors and Actuators A, vol. 133, 2007, pp. 27-34.

[11] J. J. Park and G. S. Kim, "Development of the 6-axis force/moment sensor for an intelligent robot's gripper," Sensors and Actuators A vol. 118, 2005, pp. 127-134.